American Mineralogist, Volume 71, pages 1071–1075, 1986

Quartz-phlogopite-liquid equilibria and origins of charnockites

JAMES A. GRANT
Department of Geology, University of Minnesota, Duluth, Minnesota 55812, U.S.A.

ABSTRACT

Published experimental data for quartz + K-feldspar + phlogopite + enstatite + liquid + vapor suggest that the liquid in the low-pressure invariant assemblage has less than 3 wt% H_2O, and that a thermal divide exists on the liquidus below 5 kbar. With addition of CO_2 to the system, the thermal divide persists to at least 15 kbar. The small but not negligible solubility of CO_2 in the silicate liquids apparently results in (1) a temperature range of 50–100 degrees over which quartz + K-feldspar + phlogopite + enstatite can coexist with liquid in the absence of vapor and (2) the possibility that influx of CO_2 into a solid-phase assemblage such as quartz + K-feldspar + phlogopite can initiate partial melting. Subsequent segregation of restite from liquid could lead to the formation of charnockite with a CO_2-rich vapor and biotite granite with an H_2O-rich vapor.

INTRODUCTION

Several processes may give rise to charnockite. The principal ones are (1) removal of a melt during anatexis, leaving charnockites as restites, (2) crystallization from H_2O-undersaturated magma, and (3) granulite-facies metamorphism in the presence of CO_2-rich vapor. Relations between these processes have been discussed recently by several writers, including Newton et al. (1980), Wendlandt (1981), Newton and Hansen (1983), Friend (1985), and Grant (1985). The simplest system in which charnockites can be modeled is K_2O-MgO-Al_2O_3-SiO_2-H_2O (KMASH) involving quartz (Qtz), K-feldspar (Kfs), phlogopite (Bio), enstatite (Opx), liquid (L), and vapor (V). This paper discusses implications of experimental data on equilibria related to the generation and crystallization of melt in this system, first in the absence of CO_2, and then with CO_2 as an additional component, concluding with some consequences that may be pertinent to charnockites. As discussed briefly in Grant (1985, p. 102–103), it is argued that currently available data require a thermal maximum on the liquidus (corresponding to the degeneracy quartz + phlogopite = enstatite + liquid) at low pressures in the CO_2-absent system. This results in the vapor-absent reaction being Qtz + Kfs + Bio = Opx + L (rather than Qtz + Bio = Kfs + Opx + L). This is of the same form as the analogue in the CO_2-bearing system (Qtz + Kfs + Bio + V = Opx + L), determined by Wendlandt (1981), and a maximum is apparently much more persistent with increasing pressure in the CO_2-bearing system. The resultant model is used to discuss crystal-liquid relationships under vapor-absent, vapor-saturated, and water-saturated conditions. Of particular interest regarding charnockites is the possibility that influx of CO_2 can initiate significant partial melting at low temperatures and low activity of H_2O.

EQUILIBRIA IN THE SYSTEM KMASH

Univariant equilibria in the system KMASH involving Qtz + Kfs + Bio + Opx + L + V are shown qualitatively in Figure 1 after Luth (1967) (see also Hewitt and Wones, 1984, p. 232). The dehydration reaction, Qtz + Bio = Kfs + Opx + V, as depicted in Figure 1, is after Wood (1976). The vapor-saturated solidus reactions are Qtz + Kfs + Bio + V = L and Qtz + Kfs + Opx + V = L. Theoretically, these reactions must lie on the low-temperature side of Qtz + Kfs + V = L, but it has not been possible to distinguish this difference experimentally. Thus the two reactions [Opx] and [Bio] (designating reactions by the phases that do not participate in them) are approximated by Qtz + Kfs + V = L (Bohlen et al., 1983 and Shaw, 1963). This is compatible with the experimental results on [Opx] by Wones and Dodge (1977) and with their interpretation (1977, p. 234). The location of the water-saturated melting reaction [Kfs] has been determined by Wones and Dodge (1977) at 1, 2, and 4 kbar, and by Bohlen et al. (1983) at higher pressures, and in both situations it is given as Qtz + Bio + V = Opx + L. The vapor-absent reaction [V] is shown as Qtz + Bio = Kfs + Opx + L, at pressures at and above 5 kbar (Bohlen et al., 1983). The invariant point is shown at 825°C and 500 bars, following Shaw (1963) and the extrapolation shown in Bohlen et al. (1983, Fig. 3). [Wones and Dodge (1977) suggested the slightly higher estimate of 830–840°C at 400–500 bars.]

Let us consider what implications this has for chemographic relations between the phases involved. These may be illustrated using the liquidus diagrams for quartz-bearing assemblages, shown schematically in Figure 2. For [V] to be Qtz + Bio = Kfs + Opx + L and for [Kfs] to be Qtz + Bio + V = Opx + L, the liquid compositions must project to the *right* of the Bio-Opx join, as at [V] and [Kfs]

0003–004X/86/0910–1071$02.00

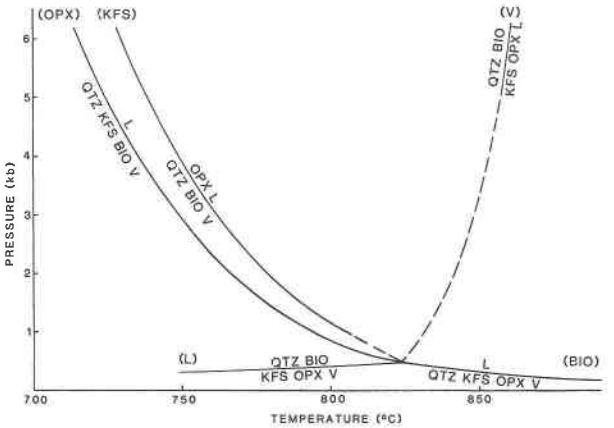

Fig. 1. Pressure-temperature grid of quartz-bearing equilibria in the system KMASH for Qtz + Kfs + Bio + Opx + L + V. [L] is from Wood (1976), [Opx] and [Bio] are approximated by Qtz + Kfs + V = L after Shaw (1963) and Bohlen et al. (1983), [Kfs] is from Wones and Dodge (1977) and Bohlen et al. (1983), and [V] from Bohlen et al. (1983). Equilibria are dashed where not explicitly defined.

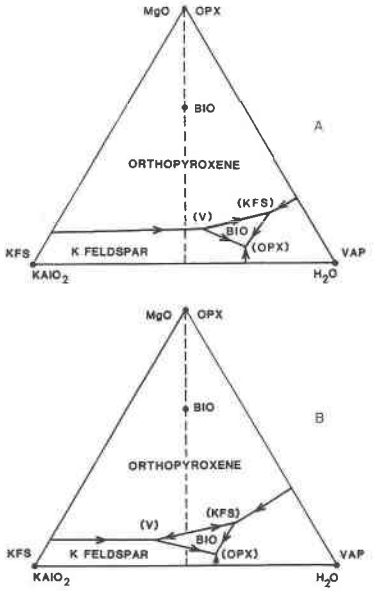

Fig. 2. Schematic isobaric liquidus diagrams for quartz-bearing assemblages in part of the system KMASH. Arrows indicate decreasing temperature. Phase compositions are plotted in mole percent, and MgO contents of liquids on the "ternary" boundary curves are exaggerated for clarity. Primary-phase fields for liquids in equilibrium with orthopyroxene, biotite, and K-feldspar are labeled. Each of these fields terminates (because the liquids become vapor-saturated) on the three boundary curves in the lower right. No silicate liquids exist to the right of these boundaries, but rather two-phase assemblages of vapor and vapor-saturated liquid. The "ternary" eutectic [Opx] is shown slightly separated from the "binary" eutectic involving Qtz + Kfs + L + V on the base of each diagram. Fig. 2A corresponds to a pressure above the invariant point of Fig. 1 or above the higher-pressure singular point of Fig. 3. Fig. 2B corresponds to a pressure between the two singular points of Fig. 3.

respectively in Figure 2A. However, the data of Tuttle and Bowen (1958) and of Shaw (1963) in the vicinity of the invariant point (Fig. 1) require that even the *water-saturated melt* in the solidus assemblage Qtz + Kfs + L + V (at the eutectic on the base of each diagram) lies to the *left* of this join. According to Shaw (1963), the liquid at 825°C and 500 bars has about 2.8 wt% H_2O, 53.5 wt% $KAlSi_3O_8$, and 43.7 wt% SiO_2. This would project on Figure 2 at $X_{KAlO_2} = 0.55$, $X_{H_2O} = 0.45$. For the same anhydrous composition, a liquid plotting at $X_{H_2O} = 0.5$ would have to have 3.5 wt% H_2O. In Tuttle and Bowen (1958, p. 54) the liquids at 500 bars are reported to contain between 2.3 and 2.9 wt% H_2O, similar to Shaw's result. [See Clemens (1984, Table 1) for a summary of the water contents of silicic to intermediate melts inferred from experiments.] These liquid compositions are not well determined, but the available data are consistent, and there is at present no compelling reason to discard them. At the invariant point, the liquids involved in each of the univariant reactions become identical, and these data indicate that the composition of this invariant liquid lies to the *left* of the Bio-Opx join. If so, in the vicinity of the invariant point, the liquids at [V], [Kfs], and [Opx] all lie on the left side of the Bio-Opx join, as is *not* shown in Figure 2.

To conform to experimental data at higher pressures, the liquid compositions must change with increasing pressure. The liquids in the water-saturated melting reactions [Opx] and [Kfs] have to move through the extended join Bio-Opx at relatively low pressure, initiating a thermal maximum on the Bio-Opx field boundary and yielding a liquidus diagram similar to Figure 2B. The liquid in the vapor-absent reaction [V] eventually follows suit, eliminating the thermal maximum and yielding a diagram similar to Figure 2A. The form of the reaction [V] changes from Qtz + Kfs + Bio = Opx + L (Fig. 2B), through the colinearity Qtz + Bio = Opx + L, to Qtz + Bio = Kfs + Opx + L (Fig. 2A).

These relationships are shown in the revised pressure-temperature grid of Figure 3 and are similar to those in the theoretical analysis of Eggler (1973). The form of the [Opx] reaction remains unchanged. However, at a low-pressure singular point, the form of [Kfs] changes from Qtz + Bio = Opx + L + V (near the invariant point) to the familiar Qtz + Bio + V = Opx + L (at higher pressure), and a thermal maximum Qtz + Bio = Opx + L is initiated. Near the invariant point the [V] reaction is Qtz + Kfs + Bio = Opx + L, but at some pressure below 5 kbar, this reaction and that of the thermal maximum terminate in a second singular point, and the reaction Qtz + Bio = Kfs + Opx + L takes their place. Note that the intersection of [V] and [Kfs] to the left of the low-pressure singular point does not generate another invariant assemblage: the compositions of the liquids lie on opposite sides of the Bio-Opx join of Figure 2B.

This interpretation fits the available experimental data

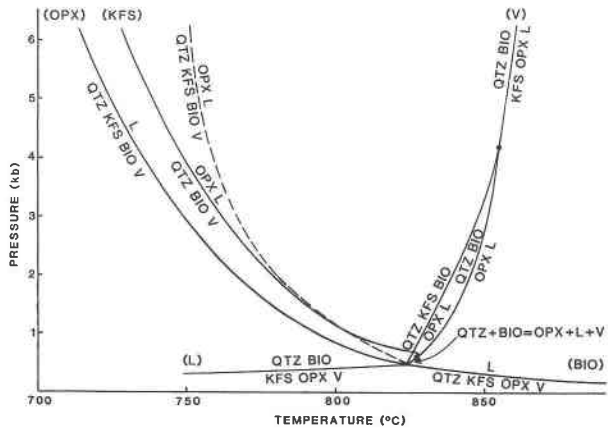

Fig. 3. Pressure-temperature grid of the equilibria of Fig. 1, revised to incorporate a thermal maximum (Qtz + Bio = Opx + L). The singular points at either end of this reaction are marked by the heavy dots. The dashed quaternary equilibrium for the system KMASH with CO_2 as an additional component (Qtz + Kfs + Bio + V = Opx + L) is from Wendlandt (1981). This must terminate in the invariant point where all six phases coexist in the CO_2-absent system.

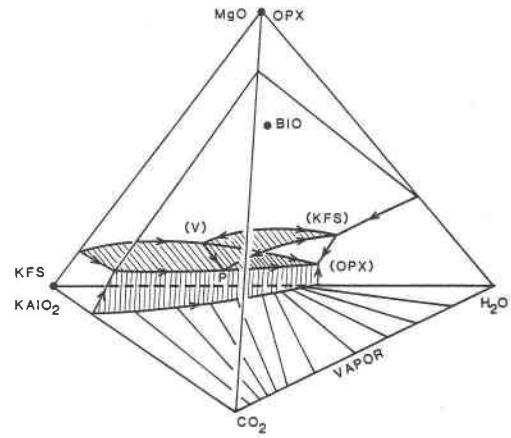

Fig. 4. Schematic isobaric liquidus diagram for quartz-bearing assemblages at a pressure of about 3 kbar, from Fig. 3. Ornamental tie lines between liquids and vapors are shown only on the base of the tetrahedron.

on the pertinent reactions in KMASH, at pressures near the invariant point and at higher pressures, including the water contents of liquids at the Qtz + Kfs + L + V solidus.

Equilibria in the system KMASH with CO_2

Let us now extend this discussion to analogous assemblages with CO_2 as an additional component. A schematic liquidus model for this is shown in Figure 4 (after Grant, 1985, Fig. 3.26). Here the rear face of the tetrahedron is the same as Figure 2B, and invariant points [Opx], [Kfs], and [V] are seen again. A primary-phase volume for biotite is flanked above by one for orthopyroxene and below by one for K-feldspar. Water vapor–saturated compositions on the liquidus are restricted to the three boundary curves on the right of the rear face, as in Figure 2B. Binary-vapor–saturated compositions on the liquidus lie on surfaces that extend from these three boundary curves, across the model in front of the three primary-phase volumes for orthopyroxene, biotite, and K-feldspar. The vapor-saturated liquidus surface for K-feldspar is shown with ruled vertical lines, the biotite surface is blank, and the orthopyroxene surface extends above these to the point on the MgO-CO_2 edge near the orthopyroxene composition. *Ornamental* tie lines are shown on the base, connecting liquids with vapors, as suggested by the work of Holloway (1976) for albite-CO_2-H_2O. The vapor-absent reaction, Qtz + Kfs + Bio = Opx + L, extends from [V] on the rear face into the tetrahedron as shown, terminating at the quaternary peritectic point *P*, corresponding to the reaction Qtz + Kfs + Bio + V = Opx + L, as reported by Wendlandt (1981). A maximum is shown on the Bio-Opx surface, which extends from the boundary curve between [V] and [Kfs] into the tetrahedron, to the point *P*.

Liquidus relations at reduced activity of H_2O, whether on the rear face (vapor-absent) or on the binary-vapor–saturated liquidus surfaces are topologically similar in this model, except within the pressure range in which liquid compositions in Qtz + Kfs + Bio + Opx + L (*P*-[V] in Fig. 4) cross to the right side of the tetrahedron. However, this is the pressure range of greatest interest. According to Bohlen et al. (1983), the [V] reaction at 5 kbar is Qtz + Bio = Kfs + Opx + L, which requires a liquid to the right of the Bio-Opx join. Thus the change in [V] must come at pressures below 5 kbar. In contrast, the quaternary reaction Qtz + Kfs + Bio + V = Opx + L, involving liquid at *P*, has been traced to at least 15 kbar by Wendlandt (1981). Thus any change to Qtz + Bio + V = Kfs + Opx + L must be at still higher pressure. The conclusion is that, with increasing pressure, [V] changes well before the quaternary equivalent *P*, as implied in Figure 3.

The available data allow us to constrain the temperatures at several of the isobaric invariant points of Figure 4, as suggested in Figure 5 for a pressure of about 3 kbar. It should be noted that the quaternary reaction (dashed in Fig. 3) is similar in temperature to the H_2O-saturated reactions and that these are well removed from the higher-temperature vapor-absent reactions. This means that the assemblage Qtz + Kfs + Bio + Opx + L has a broad stability field (50–100 degrees wide at pressures of a few kilobars) even in this restricted system. This temperature difference, owing to solubility of CO_2 in silicate liquids, is surprisingly large, but is required by the available data. [One notes that Bohlen et al. (1983, p. 271) were not able to reverse their [V] reaction, so there may be grounds for doubt about not only the location but the existence of the higher-pressure singular point.]

Whether or not the thermal divide turns out to have significant extent in the CO_2-absent system, it remains pertinent in the full system to at least 15 kbar. It permits Bio + Opx to coexist with liquids of both high and low H_2O contents. It helps to explain reaction relationships

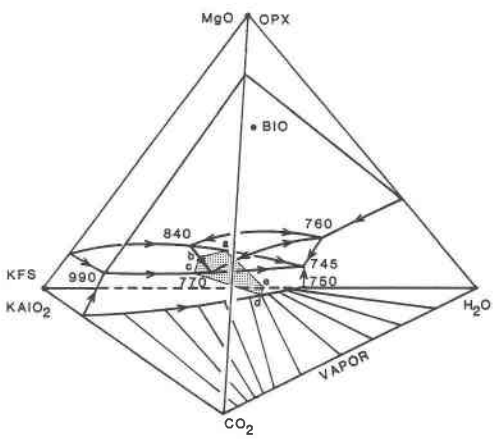

Fig. 5. Schematic isobaric liquidus diagram as in Fig. 4, with approximate temperatures of the principal isobaric invariant points shown. The dotted plane is the locus of compositions of liquids in equilibrium with quartz and K-feldspar at about 800°C.

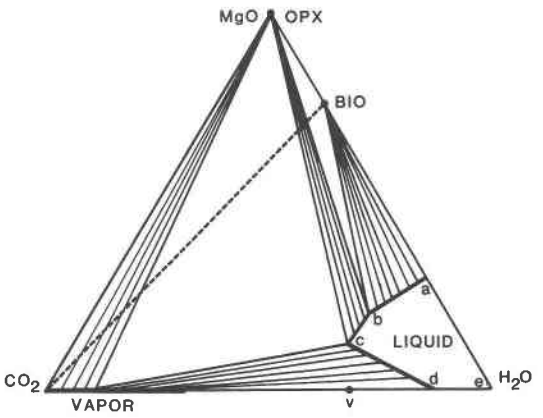

Fig. 6. Schematic projection of quartz- and K-feldspar-bearing assemblages at 800°C onto the plane MgO-CO_2-H_2O from Fig. 5. Liquid compositions (*a, b, c, d, e*) correspond to the similarly labeled points on Fig. 5; *v* is the composition of vapor derived from liquid *c* by crystallization of Bio.

such as those reported by Naney (1983) from experimental work over a range of water contents in a more complex but related system (see Grant, 1985, p. 103). But the main importance of the thermal divide is simply that it permits liquids to be in equilibrium with Qtz + Kfs + Bio + Opx at low activities of H_2O and at relatively low temperatures.

Effects of influx of CO_2

The remainder of the points to be made here do not depend on the extent of the thermal divide in the CO_2-absent system. They concern some aspects of possible relations between charnockitic assemblages, melting, and influx of CO_2. They are most readily illustrated by considering an isothermal section through the K-feldspar primary-phase volume of the tetrahedron, shown in Figure 5. The section represents the compositions of liquids in equilibrium with quartz and K-feldspar at this temperature (800°C) and pressure (3 kbar). In addition, these liquids may be in equilibrium with biotite or orthopyroxene or vapor. In particular, note at the corners of the section, the five liquids (*a, b, c, d, e*) of isothermal isobaric invariant assemblages. To avoid the horrors of working within the tetrahedron, let us project the corresponding assemblages from K-feldspar onto the front face of the tetrahedron. [This is closely analogous to isothermal isobaric projection of assemblages corresponding to a range of biotite compositions from muscovite onto the "AFM" face of the "AKFM" tetrahedron, as in Thompson (1957, Fig. 5).] The projection is shown in Figure 6, and the five liquids (*a, b, c, d, e*) project in the lower right of the diagram, tied to their several associated phases. The compositions of vapors in this projection are CO_2-rich, and only the more water-rich of these are tied to liquids, which lie between *c* and *d*.

Holding temperature and pressure constant, let us take an initial assemblage of Qtz + Kfs + Bio (plotting at Bio on Fig. 6), and add CO_2 (so that the bulk composition changes along the dashed line of Fig. 6). It is not surprising that the first thing that happens involves dehydration of the biotite. But it may be surprising that this first step is melting. This is a consequence of finite solubility of CO_2 in the liquids. As discussed above, the current experimental data imply that this may be small, but not negligible. The incongruent melting consumes Bio in favor of Opx-L_b. Application of the lever rule shows that with exhaustion of Bio, the maximum proportion of melt is produced, and the melt is that in the quaternary peritectic reaction, L_b (Fig. 5). Continued influx of CO_2 results in further dilution of the melt, which crystallizes Opx, until the melt becomes vapor-saturated and the assemblage again becomes invariant at constant pressure and temperature. This assemblage is Qtz + Kfs + Opx + L_c + V, and further CO_2 largely increases the proportion of vapor and results in crystallization of the liquid until the liquid is exhausted and all that remains is Qtz + Kfs + Opx + CO_2-rich vapor.

Let us return to the situation following saturation with vapor, with the assemblage Qtz + Kfs + Opx + L_c + V. Segregation of the liquid would leave a charnockite assemblage, Qtz + Kfs + Opx, which was in equilibrium with a high-CO_2 vapor. If we turn to the segregated liquid and allow the temperature to decrease, we can follow its evolution using Figure 5. The liquid L_c could crystallize Qtz + Kfs + Opx to the quaternary invariant point ("770" on Fig. 5). Here Bio could form and Opx be resorbed. Hereafter, crystallization of Qtz + Kfs + Bio could continue as the liquid moves toward the ternary eutectic ("745" on Fig. 5). With equilibrium crystallization, this eutectic would not be attained, because of the finite CO_2 content of L_c, which has to be accommodated in the final vapor. (The composition of this final vapor can be determined from Fig. 6, considering that we are crystallizing Bio from L_c, leaving a vapor of composition *v*.) Thus, equilibrium crystallization of L_c could yield a biotite granite in equi-

librium with a binary H_2O-rich vapor, in marked contrast to the restitic charnockite, which was in equilibrium with a binary CO_2-rich vapor.

Conclusions

1. Published experimental data in the system KMASH indicate that the liquid in the low-temperature invariant assemblage Qtz + Kfs + Bio + Opx + L + V has less than 3 wt% H_2O and that a thermal divide exists below 5 kbar. The corresponding reaction is Qtz + Bio = Opx + L. At low pressures, the vapor-absent univariant reaction is Qtz + Kfs + Bio = Opx + L, rather than Qtz + Bio = Kfs + Opx + L.

2. In the system KMASH with CO_2 as an additional component, published experimental data indicate that a thermal divide exists to at least 15 kbar and that a surprisingly large temperature difference of 50–100 degrees exists between the vapor-absent reaction in the CO_2-free system and the analogue in the CO_2-bearing system (Qtz + Kfs + Bio + V = Opx + L, Wendlandt, 1981) at pressures of a few kilobars. The thermal divide permits liquids to coexist with Qtz + Kfs + Bio + Opx at low activities of H_2O and low temperatures.

3. Protoliths composed of Qtz + Kfs + Bio ± Opx without inordinate amounts of aqueous vapor are likely to produce significant quantities of melt on or near the quaternary peritectic reaction, because there lie the low-temperature liquid compositions closest to the protolith bulk compositions.

4. Influx of CO_2 into an assemblage such as Qtz + Kfs + Bio can initiate melting. This is a consequence of the small but not negligible solubility of CO_2 in the liquid (see no. 2 above). After all the biotite is consumed and after the liquid becomes vapor-saturated, segregation of restite from liquid could lead to charnockite, which was in equilibrium with a binary CO_2-rich vapor, and biotite granite, which was in equilibrium with a binary H_2O-rich vapor.

Acknowledgments

I should like to thank Ron Frost, Bob Newton, and Penny Morton for their helpful comments on this paper. A critical but constructive review by Steve Bohlen helped improve the presentation and is much appreciated. This work was supported by National Science Foundation Grant EAR-8409664, which is gratefully acknowledged.

References

Bohlen, S.R., Boettcher, A.L., Wall, V.J., and Clemens, J.D. (1983) Stability of phlogopite-quartz and sanidine-quartz: A model for melting in the lower crust. Contributions to Mineralogy and Petrology, 83, 270–277.

Clemens, J.D. (1984) Water contents of silicic to intermediate magmas. Lithos, 17, 273–287.

Eggler, D.H. (1973) Principles of melting of hydrous phases in silicate melt. Carnegie Institution of Washington Year Book, 72, 491–495.

Friend, C.R.L. (1985) Evidence of fluid pathways through Archean crust and the generation of the Closepet granite, Karnataka, South India. Precambrian Research, 27, 239–250.

Grant, James A. (1985) Phase equilibria in partial melting of pelitic rocks. In J.R. Ashworth, Ed. Migmatites, 86–144. Blackie and Son, Glasgow.

Hewitt, D.A., and Wones, D.R. (1984) Experimental phase relations of the micas. In S.W. Bailey, Ed. Micas, 201–256. Mineralogical Society of America Reviews in Mineralogy, 13.

Holloway, J.R. (1976) Fluids in the evolution of granitic magmas: Consequences of finite CO_2 solubility. Geological Society of America Bulletin, 87, 1513–1518.

Luth, W.C. (1967) Studies in the system $KAlSiO_4$-Mg_2SiO_4-SiO_2-H_2O: I, inferred phase relations and petrologic applications. Journal of Petrology, 8, 372–416.

Naney, M.T. (1983) Phase equilibria of rock-forming ferromagnesian silicates in granitic systems. American Journal of Science, 283, 993–1033.

Newton, R.C., and Hansen, E.C. (1983) The origin of Proterozoic and late Archean charnockites—Evidence from field relations and experimental petrology. Geological Society of America Memoir 161, 167–178.

Newton, R.C., Smith, J.V., and Windley, B.F. (1980) Carbonic metamorphism, granulites and crustal growth. Nature, 288, 45–50.

Shaw, H.R. (1963) The four-phase curve sanidine-quartz-liquid-gas between 500 and 4000 bars. American Mineralogist, 48, 883–896.

Thompson, J.B., Jr. (1957) The graphical analysis of mineral assemblages in pelitic schists. American Mineralogist, 42, 842–858.

Tuttle, O.F., and Bowen, N.L. (1958) Origin of granite in the light of experimental studies in the system $NaAlSi_3O_8$-$KAlSi_3O_8$-SiO_2-H_2O. Geological Society of America Memoir 74.

Wendlandt, R.F. (1981) Influence of CO_2 on melting of model granulite facies assemblages: A model for the genesis of charnockite. American Mineralogist, 66, 1164–1174.

Wones, D.R., and Dodge, F.C.W. (1977) The stability of phlogopite in the presence of quartz. In D.G. Fraser, Ed. Thermodynamics in geology, 229–247. Reidel, Boston.

Wood, B.J. (1976) The reaction phlogopite + quartz = enstatite + sanidine + H_2O. In G.M. Biggar, Ed. Progress in Experimental petrology, 17–19. Natural Environment Research Council, Publication Series D.

Manuscript received August 7, 1985
Manuscript accepted May 16, 1986